Divergent Cytochrome *c* Maturation System in Kinetoplastid Protists

Asma Belbelazi,ᵃ Rachel Neish,ᵇ,ᶜ Martin Carr,ᵃ 🄳 Jeremy C. Mottram,ᵇ,ᶜ 🄳 Michael L. Gingerᵃ

ᵃSchool of Applied Sciences, University of Huddersfield, Huddersfield, United Kingdom
ᵇYork Biomedical Research Institute, University of York, York, United Kingdom
ᶜDepartment of Biology, University of York, York, United Kingdom

Asma Belbelazi and Rachel Neish contributed equally to this work. Author order was determined on the basis of alphabetical order.

ABSTRACT In eukaryotes, heme attachment through two thioether bonds to mitochondrial cytochromes c and c_1 is catalyzed by either multisubunit cytochrome c maturation system I or holocytochrome c synthetase (HCCS). The former was inherited from the alphaproteobacterial progenitor of mitochondria; the latter is a eukaryotic innovation for which prokaryotic ancestry is not evident. HCCS provides one of a few exemplars of *de novo* protein innovation in eukaryotes, but structure-function insight of HCCS is limited. Uniquely, euglenozoan protists, which include medically relevant kinetoplastids *Trypanosoma* and *Leishmania* parasites, attach heme to mitochondrial *c*-type cytochromes by a single thioether linkage. Yet the mechanism is unknown, as genes encoding proteins with detectable similarity to any proteins involved in cytochrome c maturation in other taxa are absent. Here, a bioinformatics search for proteins conserved in all hemoprotein-containing kinetoplastids identified kinetoplastid cytochrome c synthetase (KCCS), which we reveal as essential and mitochondrial and catalyzes heme attachment to trypanosome cytochrome c. KCCS has no sequence identity to other proteins, apart from a slight resemblance within four short motifs suggesting relatedness to HCCS. Thus, KCCS provides a novel resource for studying eukaryotic cytochrome c maturation, possibly with wider relevance, since mutations in human HCCS leads to disease. Moreover, many examples of mitochondrial biochemistry are different in euglenozoans compared to many other eukaryotes; identification of KCCS thus provides another exemplar of extreme, unusual mitochondrial biochemistry in an evolutionarily divergent group of protists.

IMPORTANCE Cytochromes c are essential proteins for respiratory and photosynthetic electron transfer. They are posttranslationally modified by covalent attachment of a heme cofactor. Kinetoplastids include important tropical disease-causing parasites; many aspects of their biology differ from other organisms, including their mammalian or plant hosts. Uniquely, kinetoplastids produce cytochromes c with a type of heme attachment not seen elsewhere in nature and were the only cytochrome *c*-bearing taxa without evidence of protein machinery to attach heme to the apocytochrome. Using bioinformatics, biochemistry, and molecular genetics, we report how kinetoplastids make their cytochromes c. Unexpectedly, they use a highly diverged version of an enzyme used for heme-protein attachment in many eukaryotes. Mutations in the human enzyme lead to genetic disease. Identification of kinetoplastid cytochrome c synthetase, thus, solves an evolutionary unknown, provides a possible target for antiparasite drug development, and an unanticipated resource for studying the mechanistic basis of a human genetic disease.

KEYWORDS cytochrome c, *Leishmania*, mitochondrial metabolism, posttranslational modification (PTM), protist, *Trypanosoma brucei*, posttranslational modification, protists
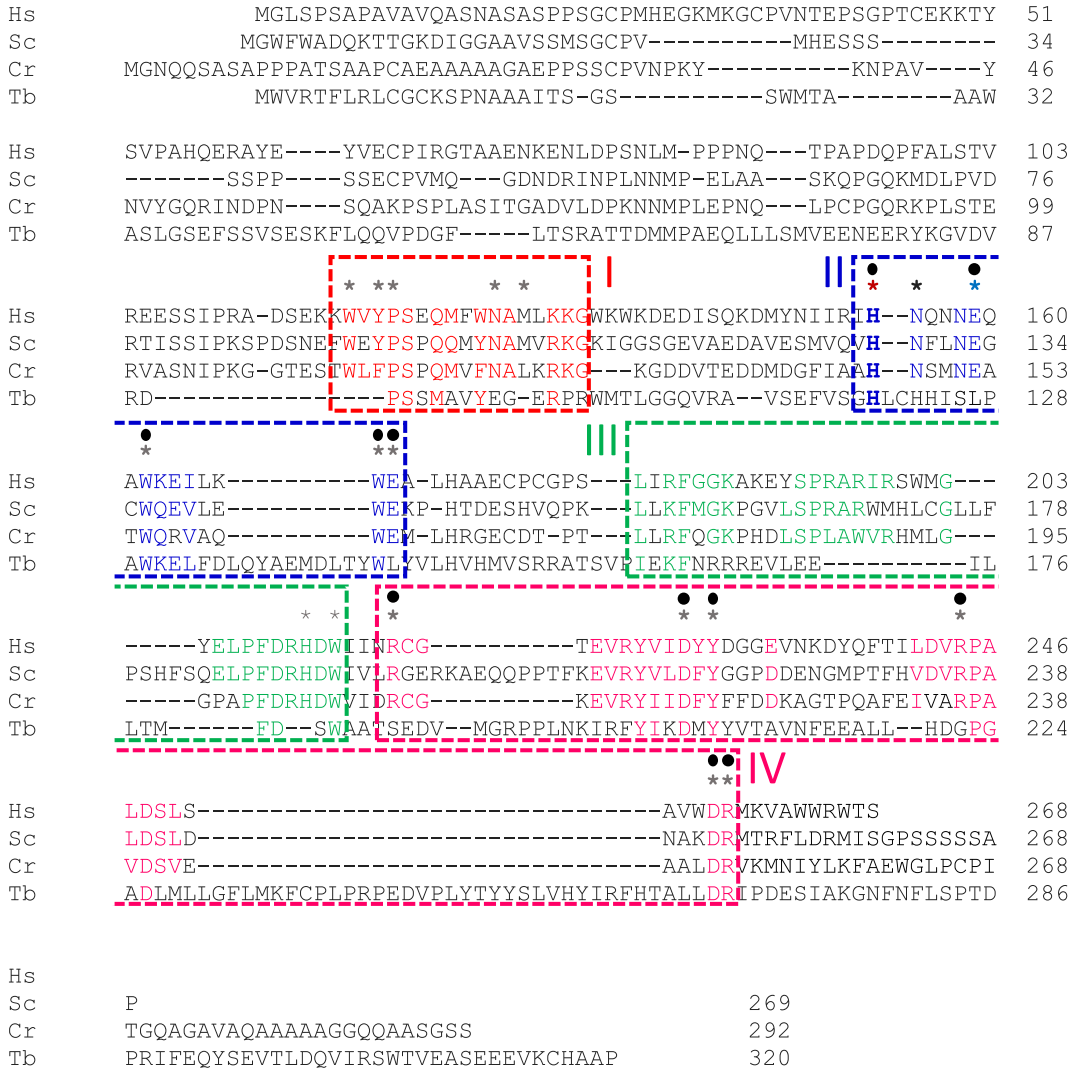
Trypanosomatid parasites of the genera *Trypanosoma* and *Leishmania* are responsible for a variety of serious neglected tropical diseases and belong to the class of flagellate protists called Kinetoplastea. Numerous aspects of kinetoplastid mitochondrial biology, including genome organization (1), RNA editing, protein/tRNA import (2), and cristae formation (3) are highly divergent or unique compared with many eukaryotes.

A fundamental aspect of mitochondrial function is covalent attachment of heme to mitochondrial cytochromes c and c_1 within the mitochondrial intermembrane space. For this posttranslational modification, thioether bonds form between heme vinyl groups and cysteine sulfhydryl groups of a CxxCH heme-binding motif within the apocytochrome. The stereochemistry of this heme attachment is conserved across evolution: the 2-vinyl group of heme attaches to the first cysteine, the 4-vinyl group attaches to the second cysteine, and histidine provides an axial ligand to the heme iron. In most eukaryotes, holocytochrome c synthetase (HCCS), associated with the outer leaflet of the mitochondrial inner membrane, catalyzes heme attachment to mitochondrial cytochromes c (4). In the protomitochondrion, however, the multisubunit, integral membrane cytochrome c maturation system I provided an ancestral pathway for c-type cytochrome biogenesis. It is retained, partially mitochondrially encoded, in many plants and a few protists. Instances of eukaryotes containing both maturation systems are extremely rare: orphan taxon and predatory flagellate *Ancoracysta twista* reportedly contains HCCS and system I but is now extinct in the laboratory (5), and a survey of the 1000 plant transcriptome resource (6) suggests that club mosses *Phylloglossum drummondii* and *Huperzia squarrosa* possess HCCS plus nuclear gene-encoded system I fragments or a mitochondrial CcmF pseudogene, respectively (A. Belbelazi, M. Carr, and M. L. Ginger, unpublished observations).
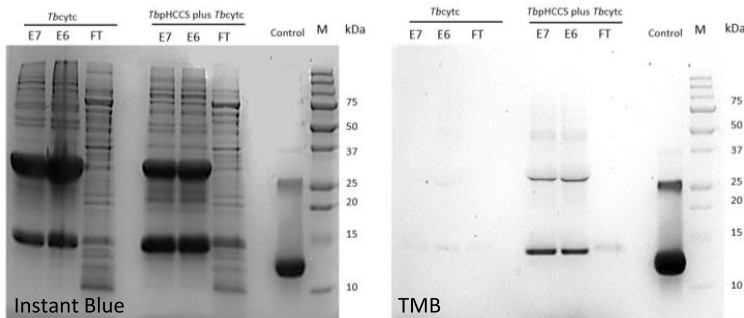
Kinetoplastid protists are the only eukaryotes where mitochondrial cytochromes are present but evidence of a cytochrome c maturation system is absent (4, 7, 8). Moreover, kinetoplastids and other euglenozoans (e.g., *Euglena gracilis*) are unique in that heme is bound through only a single thioether linkage in mitochondrial cytochromes c. In Euglenozoa, A̲AQ**C**H and F̲AP**C**H are the conserved heme-binding motifs in cytochromes c and c_1, respectively (the residue at the proximal heme-binding cysteine in normal c-type cytochromes is underlined; the heme-binding cysteine conserved in all cytochromes c is shown in bold type). Why euglenozoans possess mitochondrial cytochromes c with heme bound by a single thioether bond is a mystery of almost 50 years standing. No noticeable difference in the physicochemical properties of euglenozoan cytochromes c is known (9). Yet, the activities of *Euglena* cytochrome c reductase and oxidase vary, depending on the source of the cytochrome c used plus there are fitness costs in trypanosomes engineered to express only CxxCH heme-binding cytochrome c (10). This leaves it possible that single cysteine linkage affects electron transport through the mitochondrial respiratory chain (11). The strict conservation of phenylalanine and proline within heme-binding motifs of kinetoplastid and *Euglena* cytochrome c_1 is another puzzle and potentially unique. Perhaps, the proline introduces a local bend in the polypeptide that allows accommodation of the phenylalanine side chain within the protein's tertiary structure (11).

To resolve how kinetoplastids mature their unique mitochondrial c-type cytochromes, we sorted candidate mitochondrial proteins to identify those conserved in all kinetoplastids, except for plant-pathogenic *Phytomonas*. In *Phytomonas*, adaptation to carbohydrate-rich plant latex correlates with secondary loss of mitochondrial cytochromes and other hemoproteins (12); thus, we reasoned that in *Phytomonas*, a cytochrome c maturation system would also be lost. Candidate mitochondrial proteins were then screened for motifs similar to any present in proteins belonging to the four biogenesis systems known to catalyze heme attachment to a cysteine sulfhydryl (see Text S1 in the supplemental material). We identified a single hypothetical protein, highly conserved across the Kinetoplastea (see Fig. S1 in the supplemental material) but absent from *Phytomonas* (encoded by Tb927.3.3890 in *Trypanosoma brucei*;
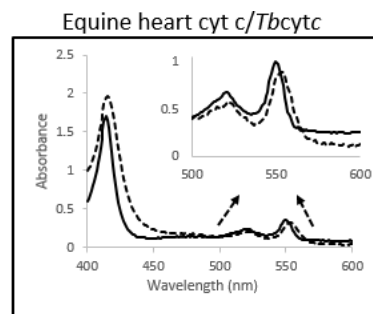
A

```
Hs              MGLSPSAPAVAVQASNASASPPSGCPMHEGKMKGCPVNTEPSGPTCEKKTY    51
Sc            MGWFWADQKTTGKDIGGAAVSSMSGCPV---------MHESSS-------    34
Cr         MGNQQSASAPPPATSAAPCAEAAAAAGAEPPSSCPVNPKY---------KNPAV----Y    46
Tb             MWVRTFLRLCGCKSPNAAAITS-GS---------SWMTA-------AAW    32

Hs         SVPAHQERAYE----YVECPIRGTAAENKENLDPSNLM-PPPNQ---TPAPDQPFALSTV   103
Sc         -------SSPP----SSECPVMQ---GDNDRINPLNNMP-ELAA---SKQPGQKMDLPVD    76
Cr         NVYGQRINDPN----SQAKPSPLASITGADVLDPKNNMPLEPNQ---LPCPGQRKPLSTE    99
Tb         ASLGSEFSSVSESKFLQQVPDGF-----LTSRATTDMMPAEQLLLSMVEENEERYKGVDV    87

Hs         REESSIPRA-DSEKKWVYPSEQMFWNAMLKKGWKWKDEDISQKDMYNIIRHH--NQNNEQ   160
Sc         RTISSIPKSPDSNEFWEYPSPQQMYNAMVRKGKIGGSGEVAEDAVESMVQVH--NFLNEG   134
Cr         RVASNIPKG-GTESTWLFPSPQMVFNALKRKG---KGDDVTEDDMDGFIAAH--NSMNEA   153
Tb         RD------------PSSMAVYEG-ERPRWMTLGGQVRA--VSEFVSGHLCHHISLP   128

Hs         AWKEILK----------WEA-LHAAECPCGPS---LIRFGGKAKEYSPRARIRSWMG---   203
Sc         CWQEVLE----------WEKP-HTDESHVQPK---LLKFMGKPGVLSPRARWMHLCGLLF   178
Cr         TWQRVAQ----------WEM-LHRGECDT-PT---LLRFQGKPHDLSPLAWVRHMLG---   195
Tb         AWKELFDLQYAEMDLTYWLYVLHVHMVSRRATSVIEKFNRRREVLEE---------IL   176

Hs         -----YELPFDRHDWLIWRCG----------TEVRYVIDYYDGGEVNKDYQFTILDVRPA   246
Sc         PSHFSQELPFDRHDWIVLRGERKAEQQPPTFKEVRYVLDFYGGPDDENGMPTFHVDVRPA   238
Cr         -----GPAPFDRHDWVIDRCG----------KEVRYIIDFYFFDDKAGTPQAFEIVARPA   238
Tb         LTM------FD--SWAATSEDV--MGRPPLNKIRFYIKDMYYVTAVNFEEALL--HDGPG   224

Hs         LDSLS-------------------------AVWDRMKVAWWRWTS   268
Sc         LDSLD-------------------------NAKDRMTRFLDRMISGPSSSSSA   268
Cr         VDSVE-------------------------AALDRVKMNIYLKFAEWGLPCPI   268
Tb         ADLMLLGFLMKFCPLPRPEDVPLYTYYSLVHYIRFHTALLDRIPDESIAKGNFNFLSPTD   286

Hs                                                           
Sc         P                                                   269
Cr         TGQAGAVAQAAAAAGGQQAASGSS                            292
Tb         PRIFEQYSEVTLDQVIRSWTVEASEEEVKCHAAP                  320
```

B

C

Equine heart cyt c/*Tbcytc*

FIG 1 (A) KCCS is a novel protein exhibiting very little sequence similarity to HCCS. MAFFT was used to align *T. brucei* (Tb) KCCS with HCCS from diverse taxa. HCCS-defining motifs I to IV are boxed. His154 is denoted by a red asterisk. Mutations seen in MLS patients are indicated by blue asterisks. Gray asterisks indicate residues analyzed by site-directed mutagenesis of *Homo sapiens* (Hs) HCCS (10, 21). Circles denote where site-directed mutation decreased HCCS activity. Cr, *Chlamydomonas reinhardtii* (XP_001697002.1); Hs, *Homo sapiens* (NP_001116080.1); Sc, *Saccharomyces cerevisiae* (NP_009361.1). NCBI reference sequences are provided in parentheses in the preceding sentence. (B and C) *Tb*KCCS-catalyzed maturation of trypanosome cytochrome *c* (*Tb*CYTC). (B) Soluble fractions from *E. coli* induced for expression (described in Text S1) of either His6-tagged *Tb*CYTC or His6-tagged *Tb*CYTC plus *Tb*KCCS from pCDFDuet-1

(Continued on next page)

LmxM.08_29.1300 in *Leishmania mexicana*) that exhibited colinearity but very limited sequence similarity to four HCCS motifs required for thioether bond formation (Fig. 1A). Similarity between this kinetoplastid protein and human HCCS was too limited to be detected by PSI-BLAST, but the histidine (His154) essential in HCCS for heme attachment to apocytochrome *c* (13) was present at an analogous position in candidate kinetoplastid cytochrome *c* synthetase (KCCS).

To assess KCCS candidature, we coexpressed recombinant Tb927.3.3890 and *T. brucei* cytochrome *c* in *Escherichia coli*. We reported previously that *T. brucei* apocytochrome *c* is neither subject to spontaneous maturation in the *E. coli* cytoplasm nor a substrate for the endogenous periplasmic *E. coli* cytochrome *c* maturation system (which is expressed minimally under the aerobic conditions we used to cultivate our *E. coli* cultures) (7). Here, recombinant expression of *T. brucei* cytochrome *c* bearing an N-terminal hexahistidine tag also resulted in no detectable holocytochrome *c* formation. Coexpression of Tb927.3.3890 and His$_6$-tagged *T. brucei* cytochrome *c*, however, resulted in heme attachment to the latter, as shown by sodium dodecyl sulfate-polyacrylamide gel electrophoresis (SDS-PAGE) of purified protein and staining for covalently bound heme (Fig. 1B). Pyridine hemochrome spectra of purified recombinant trypanosome holocytochrome *c* confirmed heme attachment via a single thioether bond (Fig. 1C): in the spectra shown, the pyridine hemeochrome α-band maximum of the recombinant cytochrome was 553 nm, and clearly red-shifted in comparison with the corresponding 550-nm α-band maximum of cytochromes *c*, which bind heme via two thioether bonds (equine cytochrome *c* in Fig. 1C). Thus, Tb927.3.3890 is appropriately referred to as *T. brucei* KCCS (Tb*KCCS*).

For molecular genetics analyses of KCCS, we used *L. mexicana* engineered for tractable CRISPR-Cas9 genome editing (denoted as T7 in Fig. 2B and T7Cas9 in Fig. 2C to E) (14). *Leishmania* promastigotes have no capacity for anaerobic growth; thus, mitochondrial cytochromes are essential (15). Tagged with mNeonGreen and expressed from an endogenous chromosomal locus, *L. mexicana* KCCS (Lm*KCCS*) showed mitochondrial localization (Fig. 2A), consistent with a role in mitochondrial cytochrome *c* maturation. Mitochondrial localization was observed irrespective of whether the mNeonGreen tag was N or C terminal, providing evidence for an internal hydrophilic mitochondrial import signal, as described in yeast HCCS (16). We were unable to generate Lm*KCCS* null mutants and were only able to delete both chromosomal copies of Lm*KCCS* without further genome rearrangements following episomal expression of green fluorescent protein (GFP)-tagged Lm*KCCS* or Tb*KCCS* (Fig. 2B to E). In the absence of pNUS-derived episomes, CRISPR-Cas9-mediated disruption of both Lm*KCCS* alleles in diploid *L. mexicana* resulted in genome duplication, as well as the site-specific integration of drug resistance cassettes, as revealed by propidium iodide (PI) staining and flow cytometry of methanol-fixed logarithmic phase parasites (Fig. 2C). Thus, CRISPR-Cas9 genome editing indicated that Lm*KCCS* is an essential gene.

Our comparative genomics approach identified KCCS and provides a mechanism by which kinetoplastids mature their mitochondrial cytochromes *c* with heme attached via a single thioether bond. Other than the missing thioether bond, X-ray structures of trypanosomatid and yeast holocytochromes *c* are very similar, although the former

FIG 1 Legend (Continued)
(Novagen) were purified by Ni^{2+} affinity chromatography. Flowthrough (FT) and elution fractions (E6 and E7) from each culture were subjected to acetone precipitation and analyzed by SDS-PAGE under nonreducing conditions. Duplicate 12% gels were stained with either Instant Blue (to confirm protein loading) or 3,3',5,5'-tetramethylbenzidine (TMB) (to detect covalent attachment of heme to protein). Fifty nanograms of equine holocytochrome *c* was loaded in the control lane of both gels. Dimerization of cytochrome *c*, evident in all lanes is explained by "domain-swapping" of the C-terminal α-helix (27) (Text S1). (C) Pyridine hemochrome spectra for recombinant trypanosome (dashed line) or equine heart cytochrome *c* (solid line) were recorded at 25°C following disodium dithionite addition. The concentration of cytochromes analyzed was 13 μM. The spectra were normalized by Soret band intensity. The inset expands the 500- to 600-nm region of the two spectra, indicating the diagnostic α-band maximum at 553 nm for cytochrome *c* with heme bound by a single thioether bond, red-shifted relative to the 550-nm α-band maximum for cytochrome *c* with a CxxCH heme-binding motif. Instant blue- and TMB-stained gels of the purified cytochrome preparation used for spectroscopy are shown in Fig. S2 in the supplemental material.
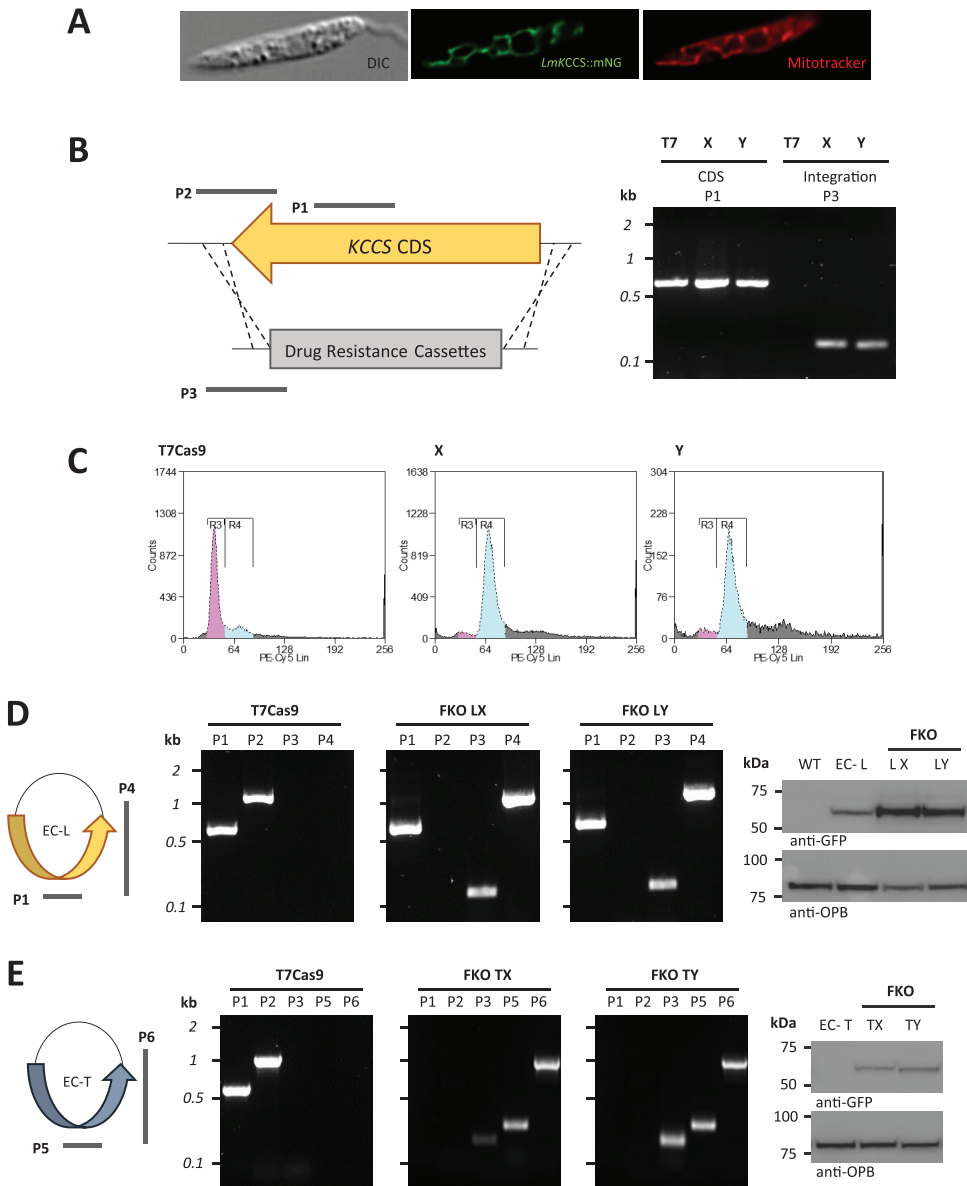
FIG 2 (A) Mitochondrial localization of Lm*KCCS*::mNeonGreen in live, CyGEL-immobilized *L. mexicana*. DIC, differential interference contrast. (B to E) CRISPR-Cas9 genome editing of *L. mexicana* reveals that Lm*KCCS* is an essential gene. (B) Homologous recombination of drug resistance cassettes into Lm*KCCS* loci with amplicons from PCR-mapping indicated. P1, amplicon within the Lm*KCCS* coding sequence (CDS); P2, downstream and within Lm*KCCS*; P3, downstream of Lm*KCCS* and within *PUR* or *BSD* resistance cassettes. Diagnostic PCR from genomic DNA (gDNA) templates extracted from *Leishmania* populations (X and Y) after transfection with single guide DNA (sgDNA) and template donor DNA for CRISPR-Cas9 gene editing. (C) Analysis of DNA content in propidium iodide-stained cell populations T7Cas9, X, and Y by flow cytometry. (D and E) Episomal expression of Lm*KCCS*::GFP (EC-L) with PCR amplicons for P1 and P4 (D) or episomal expression of Tb*KCCS*::GFP (EC-T) and PCR amplicons for P5 and P6 indicated (E). Also shown, PCR mapping of T7Cas9 parental *L. mexicana* and facilitated knockout (FKO) clones LX and LY (D) or TX and TY (E) together with immunoblot analysis of Lm*KCCS*::GFP or Tb*KCCS*::GFP expression in wild-type *L. mexicana*, episome-transfected *L. mexicana*, and FKO clones. For the loading control on the immunoblots, expression of oligopeptidase B (anti-OPB) was detected. WT, wild type.

(with either AxxCH or an engineered CxxCH heme-binding motif) is a very poor substrate for yeast HCCS (17), presumably because HCCS requires interaction with amino acids upstream of the heme-binding motif (18, 19).

The inability to detect proteins homologous to KCCS outside of the Kinetoplastea suggests that KCCS is more likely to be an extreme or highly divergent HCCS, rather

than derived through convergent evolution. Yet, irrespective of its origin, KCCS provides another example of "extreme biology" within a group of protists already well-known for pushing the boundaries (20).

Further characterization should indicate whether the amino acid differences and insertions observed in *Perkinsela* KCCS reflect this taxon's basal position in kinetoplastid phylogenies or the particular, unusual niche occupied by this obligate symbiont of *Paramoeba* (21). There is also wider significance to our observations: HCCS mutation in humans causes microphthalmia with linear skin lesions (MLS) (22, 23), but insight into HCCS catalysis, and thus the mechanistic consequence(s) of HCCS mutation, are in their infancy (13, 24–26). Our earlier work replacing "AxxCH" cytochrome *c* in *T. brucei* with a "CxxCH" variant and characterizing the resultant incorrectly matured cytochrome (10) indicates that KCCS is a highly diverged HCCS that cannot act on the first cysteine of a conventional CxxCH heme-binding motif. Indels, deletions, and substitutions within motifs I and II of KCCS, including substitution of the Glu159 MLS mutation (22), may be particularly informative for future study of HCCS catalysis, since these are the motifs believed to mediate heme binding and release (13, 26). Intriguingly, Arg217, the other residue mutated in MLS patients is also not conserved in KCCS.

Detailed methods are available in Text S1 in the supplemental material.

SUPPLEMENTAL MATERIAL

Supplemental material is available online only.
TEXT S1, DOCX file, 0.04 MB.
FIG S1, PDF file, 0.3 MB.
FIG S2, PDF file, 0.5 MB.

ACKNOWLEDGMENTS

REFERENCES

1. Aphasizheva I, Alfonzo J, Carnes J, Cestari I, Cruz-Reyes J, Göringer HU, Hajduk S, Lukeš J, Madison-Antenucci S, Maslov DA, McDermott SM, Ochsenreiter T, Read LK, Salavati R, Schnaufer A, Schneider A, Simpson L, Stuart K, Yurchenko V, Zhou ZH, Zíková A, Zhang L, Zimmer S, Aphasizhev R. 2020. Lexis and grammar of mitochondrial RNA processing in trypanosomes. Trends Parasitol 36:337–355. https://doi.org/10.1016/j.pt.2020.01.006.

2. von Känel C, Muñoz-Gómez SA, Oeljeklaus S, Wenger C, Warscheid B, Wideman JG, Harsman A, Schneider A. 2020. Homologue replacement in the import motor of the mitochondrial inner membrane of trypanosomes. Elife 9:e52560. https://doi.org/10.7554/eLife.52560.

3. Kaurov I, Vancová M, Schimanski B, Cadena LR, Heller J, Bílý T, Potěšil D, Eichenberger C, Bruce H, Oeljeklaus S, Warscheid B, Zdráhal Z, Schneider A, Lukeš J, Hashimi H. 2018. The diverged trypanosome MICOS complex as a hub for mitochondrial cristae shaping and protein import. Curr Biol 28:3393–3407.e5. https://doi.org/10.1016/j.cub.2018.09.008.

4. Babbitt SE, Sutherland MC, San Francisco B, Mendez DL, Kranz RG. 2015. Mitochondrial cytochrome *c* biogenesis: no longer an enigma. Trends Biochem Sci 40:446–455. https://doi.org/10.1016/j.tibs.2015.05.006.

5. Janouškovec J, Tikhonenkov DV, Burki F, Howe AT, Rohwer FL, Mylnikov AP, Keeling PJ. 2017. A new lineage of eukaryotes illuminates early mitochondrial genome reduction. Curr Biol 27:3717–3724. https://doi.org/10.1016/j.cub.2017.10.051.

6. One Thousand Plant Transcriptomes Initiative. 2019. One thousand plant transcriptomes and the phylogenomics of green plants. Nature 574:679–685. https://doi.org/10.1038/s41586-019-1693-2.

7. Allen JWA, Ginger ML, Ferguson SJ. 2004. Maturation of the unusual single-cysteine (XXXCH) mitochondrial *c*-type cytochromes found in trypanosomatids must occur through a novel biogenesis pathway. Biochem J 383:537–542. https://doi.org/10.1042/BJ20040832.

8. Allen JW, Jackson AP, Rigden DJ, Willis AC, Ferguson SJ, Ginger ML. 2008. Order within a mosaic distribution of mitochondrial *c*-type cytochrome biogenesis systems. FEBS J 275:2385–2402. https://doi.org/10.1111/j.1742-4658.2008.06380.x.

9. Pettigrew GW, Aviram I, Schejter A. 1975. Physicochemical properties of two atypical cytochromes *c*, *Crithidia* cytochrome *c*-557 and *Euglena* cytochrome *c*-558. Biochem J 149:155–167. https://doi.org/10.1042/bj1490155.

10. Ginger ML, Sam KA, Allen JWA. 2012. Probing why trypanosomes assemble atypical cytochrome *c* with an AxxCH haem-binding motif instead of CxxCH. Biochem J 448:253–260. https://doi.org/10.1042/BJ20120757.

11. Priest JW, Hajduk SL. 1992. Cytochrome *c* reductase purified from *Crithidia fasciculata* contains an atypical cytochrome c_1. J Biol Chem 267:20188–20195. https://doi.org/10.1016/S0021-9258(19)88685-4.

12. Kořený L, Sobotka R, Kovářová J, Gnipová A, Flegontov P, Horváth A, Oborník M, Ayala FJ, Lukeš J. 2012. Aerobic kinetoplastid flagellate *Phytomonas* does not require heme for viability. Proc Natl Acad Sci U S A 109:3808–3813. https://doi.org/10.1073/pnas.1201089109.

13. San Francisco B, Bretsnyder EC, Kranz RG. 2013. Human mitochondrial cytochrome *c* synthase's heme binding, maturation determinants, and complex formation with cytochrome *c*. Proc Natl Acad Sci U S A 110:E788–E797. https://doi.org/10.1073/pnas.1213897109.

14. Beneke T, Madden R, Makin L, Valli J, Sunter J, Gluenz E. 2017. A CRISPR Cas9 high-throughput genome editing toolkit for kinetoplastids. R Soc Open Sci 4:170095. https://doi.org/10.1098/rsos.170095.

15. van Hellemond JJ, van der Meer P, Tielens AG. 1997. *Leishmania infantum* promastigotes have a poor capacity for anaerobic functioning and depend mainly on respiration for their energy generation. Parasitology 114:351–360. https://doi.org/10.1017/S0031182096008591.

16. Diekert K, Kispal G, Guiard B, Lill R. 1999. An internal targeting signal directing proteins into the mitochondrial intermembrane space. Proc Natl Acad Sci U S A 96:11752–11757. https://doi.org/10.1073/pnas.96.21.11752.

17. Fülöp V, Sam KA, Ferguson SJ, Ginger ML, Allen JWA. 2009. Structure of a trypanosomatid mitochondrial cytochrome *c* with heme attached via only one thioether bond and implications for the substrate recognition

requirements of heme lyase. FEBS J 276:2822–2832. https://doi.org/10.1111/j.1742-4658.2009.07005.x.

18. Zhang Y, Stevens JM, Ferguson SJ. 2014. Substrate recognition of holocytochrome *c* synthase: N-terminal region and CXXCH motif of mitochondrial cytochrome *c*. FEBS Lett 588:3367–3374. https://doi.org/10.1016/j.febslet.2014.07.026.

19. Babbitt SE, Hsu J, Kranz RG. 2016. Molecular basis behind inability of mitochondrial holocytochrome *c* synthase to mature bacterial cytochromes: defining a critical role for cytochrome *c* α helix-1. J Biol Chem 291:17523–17534. https://doi.org/10.1074/jbc.M116.741231.

20. Butenko A, Hammond M, Field MC, Ginger ML, Yurchenko V, Lukeš J. 2020. Reductionist pathways for parasitism in euglenozoans? Expanded datasets provide new insights. Trends Parasitol 37:100−116. https://doi.org/10.1016/j.pt.2020.10.001.

21. Tanifuji G, Cenci U, Moog D, Dean S, Nakayama T, David V, Fiala I, Curtis BA, Sibbald SJ, Onodera NT, Colp M, Flegontov P, Johnson-MacKinnon J, McPhee M, Inagaki Y, Hashimoto T, Kelly S, Gull K, Lukeš J, Archibald JM. 2017. Genome sequencing reveals metabolic and cellular interdependence in an amoeba-kinetoplastid symbiosis. Sci Rep 7:11688. https://doi.org/10.1038/s41598-017-11866-x.

22. Wimplinger I, Shaw GM, Kutsche K. 2007. HCCS loss-of-function missense mutation in a female with bilateral microphthalmia and sclerocornea: a novel gene for severe ocular malformations? Mol Vis 13:1475–1482.

23. Wimplinger I, Morleo M, Rosenberger G, Iaconis D, Orth U, Meinecke P, Lerer I, Ballabio A, Gal A, Franco B, Kutsche K. 2006. Mutations of the mitochondrial holocytochrome *c*-type synthase in X-linked dominant microphthalmia with linear skin defects syndrome. Am J Hum Genet 79:878–899. https://doi.org/10.1086/508474.

24. Babbitt SE, San Francisco B, Bretsnyder EC, Kranz RG. 2014. Conserved residues of the human mitochondrial cytochrome *c* synthase mediate interactions with heme. Biochemistry 53:5261–5271. https://doi.org/10.1021/bi500704p.

25. Mendez DL, Babbitt SE, King JD, D'Alessandro J, Watson MB, Blankenship RE, Mirica LM, Kranz RG. 2017. Engineered holocytochrome *c* synthases that biosynthesize new cytochromes *c*. Proc Natl Acad Sci U S A 114:2235–2240. https://doi.org/10.1073/pnas.1615929114.

26. Babbitt SE, Hsu J, Mendez DL, Kranz RG. 2017. Biosynthesis of single thioether *c*-type cytochromes provides insight into mechanisms intrinsic to holocytochrome *c* synthase (HCCS). Biochemistry 56:3337–3346. https://doi.org/10.1021/acs.biochem.7b00286.

27. Hirota S, Hattori Y, Nagao S, Taketa M, Komori H, Kamikubo H, Wang Z, Takahashi I, Negi S, Sugiura Y, Kataoka M, Higuchi Y. 2010. Cytochrome *c* polymerization by successive domain swapping at the C-terminal helix. Proc Natl Acad Sci U S A 107:12854–12859. https://doi.org/10.1073/pnas.1001839107.